Journal of Applied Polymer Science

Cure Monitoring of Epoxy Films by Heatable *In Situ* FTIR Analysis: Correlation to Composite Parts

Ulrike Braun, Kerstin Brademann-Jock, Wolfgang Stark
BAM Federal Institute for Materials Research and Testing, Unter den Eichen 87, 12200 Berlin, Germany
Correspondence to: U. Braun (E-mail: ulrike.braun@bam.de)

ABSTRACT: The curing mechanism of an epoxy film containing dicyandiamide (DICY) and an epoxy formulation based on diglycidyl ether of Bisphenol A (DGEBA) polymer was studied as a function of various temperature programs. The investigation was performed *in situ*, using a thin film of the epoxy mixture on a silicon wafer substrate in a heatable transmission tool of a FTIR spectrometer. Based on these model-curing experiments, a major curing mechanism was proposed, taking into account the appearance, the decrease, and the development of characteristic bands at various temperatures. The conclusions of the model curing were correlated to FTIR measurements on a real, 50-mm-thick glass fiber reinforced component composite part from a technical process. It could be shown that characteristic bands that develop at curing temperatures above 150°C appear especially in the center of the thick sample. From the chemical or molecular point of view, this demonstrates the established technician's understanding that temperature control inside a large-scale fiber composite of, for example, aircraft, wind-turbine, automotive applications component is of major importance. © 2013 Wiley Periodicals, Inc. J. Appl. Polym. Sci. **2014**, *131*, 39832.

KEYWORDS: crosslinking; resins; spectroscopy; thermosets; thermal properties

Received 16 April 2013; accepted 8 August 2013
DOI: 10.1002/app.39832

INDRODUCTION

The cure monitoring of epoxy resins and prepregs is a user-orientated problem. The optimization and quality control of a curing program for complex, large-scale epoxy-composite structures with various mechanical loads, such as for wind turbines or aerospace/automotive parts, is important due to the cost of the process (in energy and time) and the durability of the material (mechanics). For practical purposes, it is common to monitor the relevant mechanical material or product characteristics,[1–3] instead to analyze the complex physical and chemical processes influencing the curing reaction of large-scale specimens. The analysis of these physicochemical parameters, such as crosslinking kinetics, viscosity, and micromechanics[4–8] is an area for intensive practice-related research. The additional use of chemical analytics tools, such as infrared and Raman spectroscopy and high-pressure liquid chromatography, is also established as a way to understand the chemical reaction of the curing process.[9–13]

In this article, we want to investigate the chemical reactions that take place during curing and correlate them to praxis. According to the literature, the temperature in the center of large-scale construction parts during the curing process can exceed the temperature of the mold.[1,3] This is caused by the heat flow of the exothermic reaction during the crosslinking reaction and the deteriorated temperature transport in the material. Therefore, we analyzed *in situ* the chemistry of resin during curing up to the start of decomposition. The results obtained were correlated to practical applications, namely, to a composite bar specimen cured in a large-scale compressing mold.

To analyze the chemistry, we used an *in situ* heatable infrared tool and observed the curing process of a thin film *in situ* at various temperature profiles. In contrast to more common cure-monitoring tools, such as differential scanning calorimetry (DSC), rheology, and ultrasonic measurements, in the infrared spectroscopy, reactive bonds are measured, independent of their contribution to a material characteristic. This means that the infrared analysis can provide the curing degree of a material, but does not give absolute information, for example, about the glass transition temperature or the E' modulus. On the other hand, infrared analysis can give insight into the chemical reactivity of the epoxy mixture. The *in situ* cure monitoring of epoxies or reactive components by nearinfrared or midinfrared tools as well as Raman spectroscopy[9,12–15] is described; however, a detailed understanding of the studied materials is still lacking.

The material we use in this study is an epoxy mixture of a resin based on diglycidyl ether of Bisphenol A (DGEBA) polymer and a hardener based on dicyandiamide (DICY). It is well established that the crosslinking reaction of the oxiran ring of resin

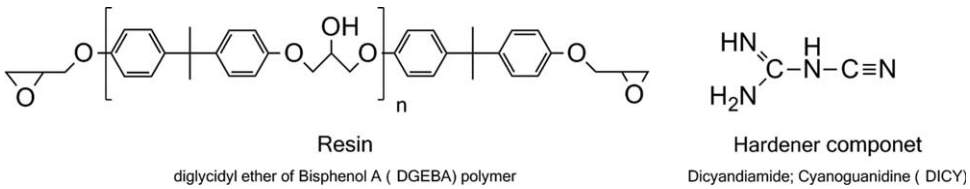

Figure 1. Chemical structure of the major components used.

with the primary amine group of the hardener occurs first.[10,14,16–20] But different mechanisms come to bear in the further progress of curing. In some works, the intra-molecular reaction to an imidazolidinone or oxazolidinone derivative is preferred,[10,17,19] while in others, the intermolecular reaction with further oxygen groups from formed hydroxyl groups or oxygen from residual water or solvents are considered.[17–20] The latter results in the formation of an iminoether, which will rearrange to an urea derivative.

EXPERIMENTAL

Methods

The Fourier transform infrared (FTIR) investigations of solids were performed using attenuated total reflection (ATR) or transmission mode in a Nicolet 6700 FTIR spectrometer (Thermo Scientific) with a deuterated-triglycine-sulfate detector with potassium bromide window (DTGS KBr). Thirty-two scans were taken at an optical resolution of 4 cm^{-1}. For reproducible test, results at least three measurements were taken for each type. The wavenumbers in the text are accurate to $\pm$ 3 cm^{-1}.

For ATR measurements (Smart Orbit Accessory), the samples were fixed on the crystal to obtain surface-sensitive spectra. The resulting spectra were ATR-corrected.

Continuous FTIR measurements in the condensed phase (one spectra takes 31 s) were carried out using a enclosed vertical, heatable FTIR device in transmission mode (FTIR 600, Linkam Scientific Instruments) in the FTIR spectrometer. Measurements were performed under nitrogen and under air. The heating rate was 2 K min^{-1} and the gas-flow rate inside the Linkam cell was 100 mL min^{-1} from 30 up to 300 °C. For the measurements, epoxy films were prepared on silicon wafers. Silicon wafers were chosen as substrate material because they are readily available and less expensive than potassium bromide or sodium chloride windows. The wafers were cleaned with acetone before use and the transparency of the wafer was checked for the applied temperature range. The measurements were performed in transmission mode; therefore, only peaks with extinctions of less than one were considered in the evaluation.

The FTIR microscope measurements were done with an IR HYPERION 3000 microscope (Bruker) with a mercury-cadmium-telluride detector (MCT). Areas in transmission mode were analyzed with a dimension of 170 $\times$ 170 μm^2, and 32 scans performed at an optical resolution of 4 cm^{-1}. Peaks with extinctions of less than two were considered in this evaluation.

The differential scanning calorimetric measurements (DSC, Netzsch 204-F1 Phoenix) were made in a temperature range from 0 up to 250°C, using a heating rate of 10 K min^{-1} and sample masses of 15–20 mg in perforated aluminum pans.

Thermal decomposition of the materials was investigated by means of thermogravimetric analysis (TGA/SDTA 851, Mettler Toledo). Measurements were performed from 30 up to 600°C under nitrogen with a heating rate of 10 K min^{-1} and a gas flow rate of 30 mL min^{-1}. The sample masses were 10 mg and alumina pans were used.

The sampling from the real specimen was done with a microtome (Leica CM 1950).

Materials

All materials are commercial used, standard components, optimized for their practical application due to processing and final performance. Three components were provided by industry partner: a pot of the resin, a pot of the hardener, and a pot of the accelerator.

The used resin consist of diglycidyl ether of Bisphenol A polymer (Figure 1). The dimension of *n* in the resin was not analyzed in the work and will not be considered, because it will not influence the reaction of oxiran rings with nitrogen groups of the hardener. However, with reference measurements at standard materials, the dimension of *n* was estimated. The dimension of *n* in our resin is not zero, because the specific oxiran ring signal at 915 cm^{-1} is decreased and the secondary hydroxyl signals around 3500 and 1110 cm^{-1} are increased compared to neat Bisphenol A diglycidyl ether (Sigma Aldridge, D 3415, epoxy content = 5.86 equiv kg^{-1}) and established epoxy resin materials such as Araldite LY 556 (Huntsman, epoxy content = 5.30–5.45 equiv kg^{-1}). We determine the peak area from oxiran ring signal (928–885 cm^{-1}) of both reference materials and extrapolate the linear dependency to our resin. According to our evaluation an epoxy content of 5.00 equiv kg^{-1} results.

The used hardener based on dicyandiamide (Figure 1), diluted in diglycidyl ether of Bisphenol A polymer. The accelerator was also diluted in diglycidyl ether of Bisphenol A polymer. The accelerator is in practice an aryl and/or alkyl urea or carbonyldiimidazole.[21,22] An exact concentration of hardener and accelerator in diglycidyl ether of Bisphenol A polymer solution is not known.

The samples for the investigation of the single components were used as received. The mixtures of epoxy resin were freshly prepared before measurement. The components, that is, resin, hardener, accelerator, were mixed carefully by hand at a temperature of 60–70°C in a relative weight ratio of 100 : 15 : 5. This composition was chosen according to the industrial application. For the *in situ* FTIR measurements, the resulting high-viscose

Table I. Overview of the Investigated Samples, the Preparation of Samples, and Methods Used

Investigated samples	Composition	Sample preparation	Applied investigation
Accelerator	Urea or carbonyldiimidazole[a]	As received	ATR-FTIR
Hardener	DICY[a]	As received	ATR-FTIR, TGA
Noncured mixture	DICY/DGEBA/Accelerator	Freshly prepared	ATR-FTIR, TGA, DSC, Trans-FTIR
Cured mixture	DICY/DGEBA/Accelerator	Freshly prepared and cured in oven for 2 h at 140°C	ATR-FTIR, TGA
Real sample (RS)	DICY/DGEBA/Accelerator/ glass fibers	Microtome cuts from industrially cured bar specimen	IR microscope, TGA

[a] Dissolved in diglycidyl ether of Bisphenol A polymer.

paste was spread on substrate windows at room temperature. As a reference, samples of around 5 g were cured in aluminum trays for 2 h in a ventilated oven at a temperature of 140°C.

As a real sample (RS), a 50-mm-thick composite part was taken from an industrial specimen. The bar was reinforced with around 78 wt % of glass fibers (TGA analysis under air) and cured for 1 h at 110°C with a subsequent tempering process for 2 h at 160°C. The sampling is described in detail later in the text and in Figure 9, respectively. The resulting samples after microtome cutting have a thickness between 80 and 100 μm.

An overview of the investigated samples, the composition, and preparation of samples and the applied analysis methods are given in Table I.

RESULTS AND DISCUSSION

Characterization of the Components

In Figure 2, spectrum of the noncured mixture is presented and compared to the major single components. By means of reference spectra, the hardener could be unambiguously identified as cyanoguanidine or dicyanodiamide (DICY) diluted in polymerized bisphenol A diglycidyl ether units. The resin was identified

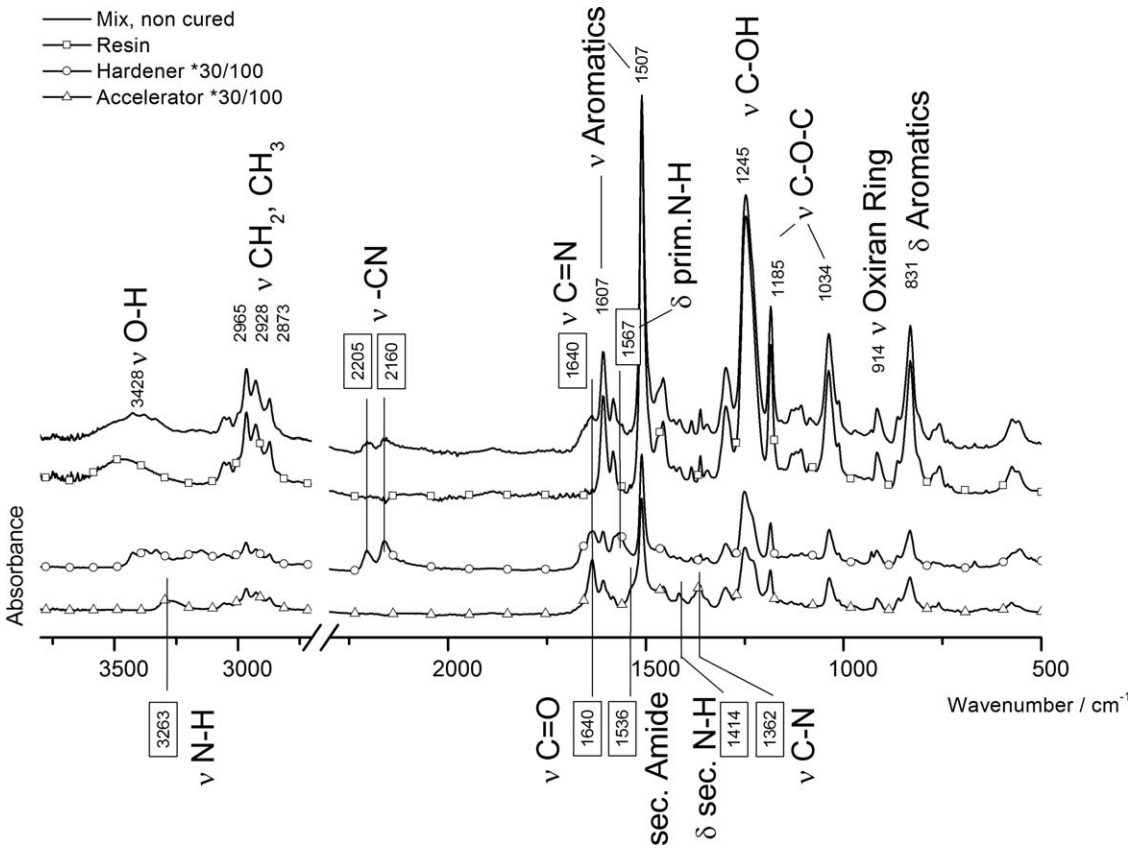

Figure 2. ATR-FTIR spectra of the single components and the noncured mixture (vertical numbers represent IR absorption frequencies in cm^{-1}). For optical reason the spectra of hardener and accelerator were minimized, the minimization is not referred to the concentration of the single species.

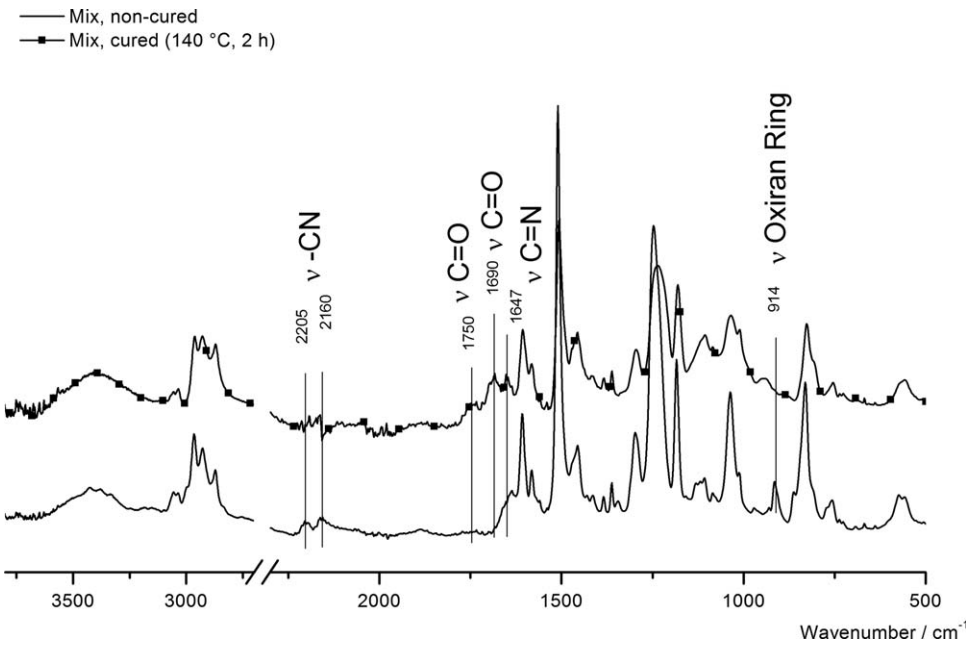

Figure 3. ATR-FTIR spectra of the noncured and the oven cured mixtures (vertical numbers represent IR absorption frequencies in cm^{-1}).

as neat polymer of diglycidyl ether of Bisphenol A. Signals of the accelerator consist also of signals from polymerized bisphenol A diglycidyl ether units in combination with additional signals.

The FTIR spectrum of the noncured mixture is dominated by the presence of the resin, in accordance with its higher content in the mixture compared to the hardener. These are the aliphatic carbon–hydrogen signals at 2965, 2928, and 2873 cm^{-1} (νCH), aromatic ring signals at 1607, 1507 (νAr) and at 830 cm^{-1} (δAr), hydroxy signals at 3428 cm^{-1} (νO—H) and 1245 cm^{-1} (νC—OH) and ether signals at 1183 and 1034 cm^{-1} (νC—O—C).[4,9,10] Clearly visible is the characteristic oxiran ring vibration at 914 cm^{-1} (νOxiran).[4,9,10,14,18,19] However, the hardener can be unambiguously identified in the mixture by signals of nitrile at 2205 and at 2160 cm^{-1} (ν-CN) as well as imine signal at 1640 cm^{-1} (νC═N) and primary amine signal at 1567 cm^{-1} (δN—H).[4,16,18,19] The splitting of nitrile signals is caused by the different tautomeric derivatives of DICY present in the molecule. By comparison with bands from organic nitrile or anorganic cyanide derivatives (database), we conclude that the band around 2205 cm^{-1} is caused by covalently bonded cyanide groups, such as those present in propionitrile (2250 cm^{-1}), benzonitril (2225 cm^{-1}), and diethyl cyanamide (2220 cm^{-1}), whereas the band around 2160 cm^{-1} is correlated with more ionically bonded cyanide species, such as those present in potassium cyanide (2080 cm^{-1}) and copper or silver cyanides (~2160 cm^{-1}). The neat accelerator is characterized by signals at 3263 cm^{-1} (νN—H), 1640 cm^{-1} (νC═O), and 1536 cm^{-1} (sec. Amide), 1414 cm^{-1} (δN—H), and 1362 cm^{-1} (νC—N), which indicated an alkyl urea. In the noncured mixture, these signals are overlapped by the higher concentrated resin and hardener. In consequence, signals of accelerator could not be identified any more. Therefore, in the further discussion, the contribution of the accelerator is neglected.

FTIR analysis of the noncured and the oven-cured mixtures (Figure 3) reveals some clear differences in the two spectra. On the one hand, bands vanished, such as the nitrile signals at 2205 and 2160 cm^{-1} as well as the oxiran ring signal at 914 cm^{-1}; on the other hand, new bands were formed, such as the signals at 1750, 1690, or 1647 cm^{-1}. The latter is attributed to newly formed imine signals, whereas the signals between 1680 and 1750 cm^{-1} are correlated with various carbonyl species, such as those present in cyclic or linear urea or urethane species.[18,19] The characteristic ether signals between 1300 and 1000 cm^{-1} change in position and intensity, indicating the formation of a newly created network with changed flexibility of various bonds.

The formation of carbonyls can also indicate oxidation on the sample surface during the curing process in the oven. This effect becomes very intensive, because the very easy-to-handle and user-friendly ATR-FTIR tool produces sensitive measurements of the specimen surface. Furthermore, the intensity of the nitrile signals is very low. This is caused by the absorption region of the ATR crystal (2300–1800 cm^{-1}), which causes a minor intensity of signals in this area of the spectra. This effect is well known, but for the majority of chemical bonds this area of the FTIR spectra is of minor importance. Therefore, the detection by *in situ* FTIR transmission mode is the better method.

Before the FTIR *in situ* measurements, the materials were initially analyzed by DSC and TGA, identifying the major curing temperature range and the onset of thermal decomposition. In the DSC, measurement [Figure 4(a)] of the noncured mixture an exothermic signal between 100 and 150°C can be detected with a maximum at 144°C. A reaction enthalpy of 334 J g^{-1} was determined. During the second heating, this signal has vanished, indicating the finished crosslinking process of resin and hardener. In the second heating, the glass transition temperature

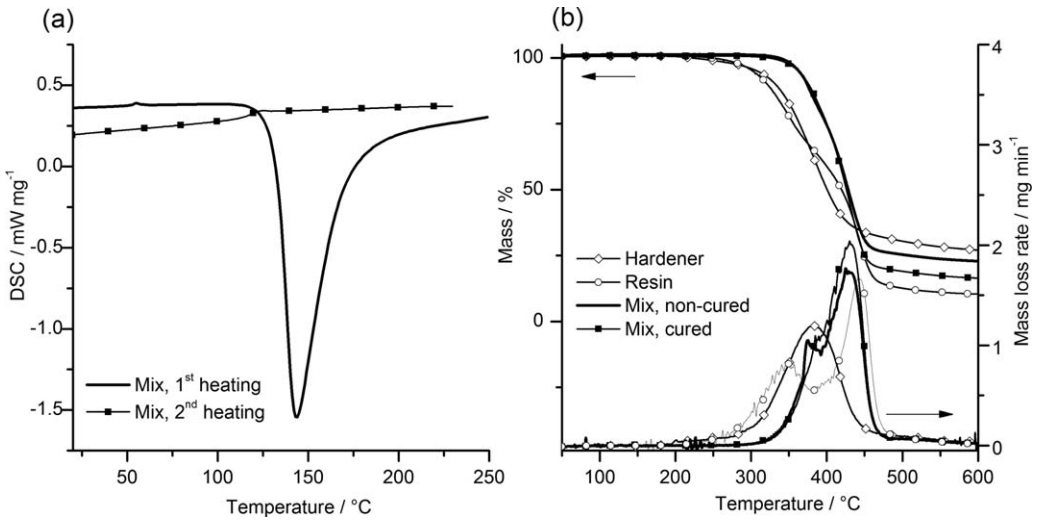

Figure 4. DSC (a) and TGA (b) measurements of the single components and the noncured and oven-cured mixtures.

($T_{g\ max}$) could be identified at around 118–120°C. By TGA analysis [Figure 4(b)], it is shown that the resin and the hardener start to decompose above 200°C. The hardener decomposes in a single decomposition step with a maximum of weight loss rate (DTG_{max}) at 384°C and a residue of 27.3 wt %. The resin decomposes in two decomposition steps with DTG_{max} at 350 and 443°C and a residue of 10.5 wt %. The mixtures also decompose in two steps. The DTG_{max} values are similar for the cured mix (388, 431°C) and the noncured mix (379, 428°C). However, the difference in the residue formation of the noncured (22.5 wt %) and the oven-cured mixtures (16.5 wt %) indicated that thermal treatment in the TGA (dynamic conditions from room temperature up to 250°C, 10 K min^{-1}) and thermal treatment in the oven (isothermal conditions at 140°C, 2 h) will not result in the same crosslinking network. But below 300°C, the materials will not decompose.

Characterization of the Model Curing Process

For the analysis of the curing process by means of FTIR, a thin film of the mixture was prepared on silicon wafer and fixed in the IR beam. Before the experiment was started, it was controlled that the intensities of the most important bands, such as the nitrile signals or the oxiran ring, did not exceed an extinction of one. Above this value, the Lambert Beer equation will no longer apply. When heating FTIR measurement tools are applied, it must always be kept in mind that FTIR spectra at higher temperatures can differ from the same spectra at room temperature. On the one hand, the overtone and combination bands could be enhanced, because they are composed differently at higher-temperature vibration levels. On the other hand, especially in this application, hydrogen bridges can open at higher temperatures, resulting in changes in the signals of the functional groups involved. Therefore, the temperature influence on the spectra has to be monitored carefully when changes are observed during curing.

Figure 5 shows selected, characteristic spectra of noncured mixture at 30, 160, and 300°C and after cooling down to room temperature (end). This experiment was performed under dynamic conditions, using a heating rate of 2 K min^{-1}. The amine or hydroxyl signals round 3428 cm^{-1} show a strong influence by the curing process and the temperature. Besides a shift in the absolute position, this signal changes in intensity. It is not clear whether this behavior is caused by changed amine and hydroxyl species or whether it is influenced by temperature effects. This means that this band is not useful for controlling the curing process *in situ*.

The oxiran ring signal at 914 cm^{-1} decreases with increasing temperature, indicating the consumption of the reactive oxiran ring with the progress of the reaction. As the frequency remains constant at 914 cm^{-1}, no influence by temperature can concluded. However, it should be noted that the oxiran ring vibration is disadvantageous for cure monitoring, because it overlaps with other signals.[14]

The nitrile bands in the mixture vanished with the curing process as expected, indicating consumption of the hardener. By reference measurement with only hardener on the substrate, it could be proved that the position of nitrile bands at 2205 and 2160 cm^{-1} are not influenced by temperature. The analysis of all individual spectra of the mixture revealed that both bands disappear continuously but a new intermediate band is formed at 2173 cm^{-1}. Whereas the band at 2205 cm^{-1} is attributed to more covalently bonded nitrile and the band at 2160 cm^{-1} is correlated to more ionically bonded cyanides, the new intermediate nitrile band must be caused by a component with averaged characteristics of both extreme positions. However, we concluded that the change in the nitrile signal indicates the increase in masses at the ends of the chemical bonds through the formation of the crosslinking network.

The imine signal at 1640 cm^{-1} decreases during curing, thus also representing the consumption of DICY. However, a slight shift in the wavenumber with temperature can be observed. Because a significant influence of hydrogen bonds on imine band can be excluded, this indicates the formation of the various intermediate species postulated for the established curing mechanism.[10,18–20] A carbonyl signal at 1690 cm^{-1} is formed

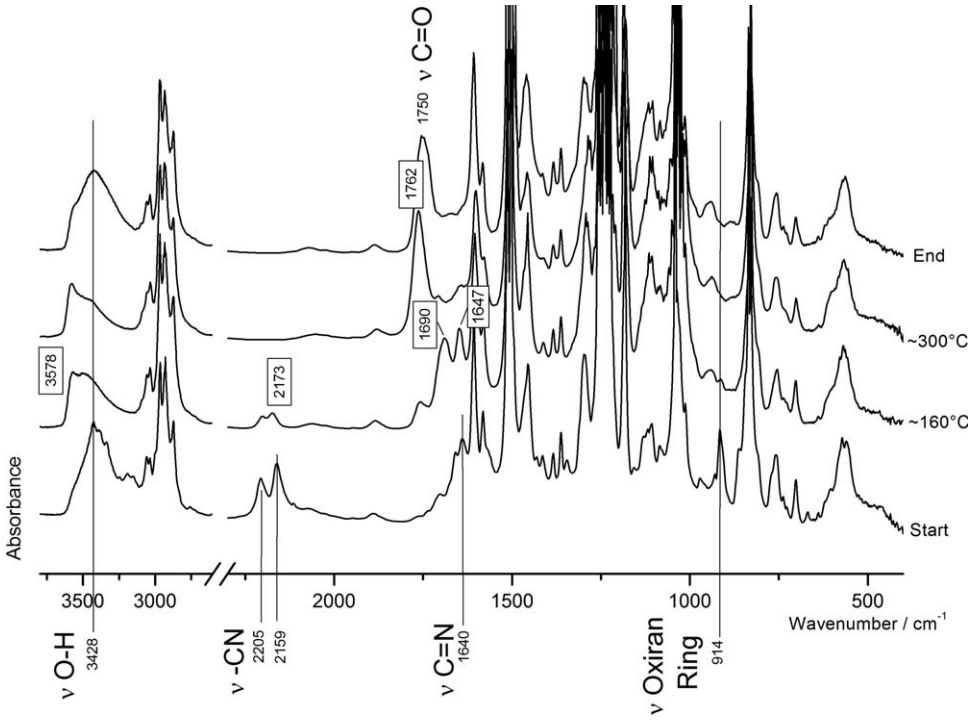

Figure 5. Selected FTIR spectra during the curing process of noncured mixture in heatable transmission cell experiment (vertical numbers represent IR absorption frequencies in cm^{-1}).

during the curing process and vanishes at higher temperatures, and finally, a carbonyl signal at 1762 cm^{-1} is formed at higher temperatures. The shift to a wavenumber of 1750 cm^{-1} after cooling the sample illustrates the effect of temperature. Whereas the band around 1700 cm^{-1} is attributed to carbonyl bands in urea species, the band at 1762 cm^{-1} (1750 cm^{-1}, respectively) is correlated with carbonyl bands in urethane structures.

In Figure 6, the curing process is evaluated by signal intensity integration versus temperature program. The temperature program is illustrated on top and the run of characteristic signals, such as nitrile, oxiran, amine, and carbonyl bands. On the left of Figure 6, the dynamic measurement is shown, on the right a measurement with isothermal steps. The program with isothermal steps is a characteristic for industrial curing procedure of an epoxy composite material. The temperature range up to 80°C is cutoff, because up to this point the film softens and thus changes the signal intensity, probably as a consequence of changes in the film thickness. The integration parameters for these evaluations are summarized in the middle column of Table II. A reference peak was not considered in the evaluation, because the spectra were continuously taken from the same position in the sample. Unfortunately, the signal of carbonyl at 1690 cm^{-1} and the imine band at 1640 cm^{-1} could not be separated due to the shift in the bands by temperature. Therefore, both signals are summarized in one evaluation. In the further discussion, only the urea carbonyl will be considered, because this peak developed more significantly during the curing process. Similarly, no distinction could be made among the various nitrile signals.

As expected from the discussion of the individual spectra, the intensity of the oxiran and the nitrile signals decreases with curing time (see also Figure 5). This is caused by the consumption of both reactive species according to the curing process. The majority (two-third) of both species reacts up to 110°C, with the residual amount of the molecules reacting up to the end of experiment. In the isothermal experiment, a slightly higher amount of the nitrile signal remains than in the dynamic experiment. This is probably caused by the formation of the intermediate nitrile band that formed at around 2173 cm^{-1}.

The urea carbonyl signal decreases up to a certain point; afterwards it increases. For the dynamic experiment, a subsequent decrease can be observed above 200°C. This decrease goes along with a strong increase in the urethane carbonyl signal. The formation rate of urethane carbonyl starts from negative values. Since this is only a mathematical effect, the signal can be neglected below 150°C. But above 150°C, the signal increase becomes significant. According to both measurements, it can be concluded that the urea carbonyl turns into urethane carbonyl at temperatures above 200°C.

Based on the results a major curing reaction pathway was formulated (Figure 7). At first, the oxiran ring will react with the primary amines of the hardener (Initial crosslinking). After consumption of all primary amines, the secondary amines and the formed hydroxyl group will react further with oxiran rings. This process will stop when all oxiran rings are consumed. Through these reactions each oxiran ring forms a crosslinking point. Afterward, the chains will further crosslink by reaction of the hydroxyl groups with the nitrile group (Further crosslinking). This reaction can be observed in the decreased intensity of the nitrile signal at 2173 cm^{-1}. Carbonyl bands of urea derivatives are formed, which are caused by the rearrangement of the

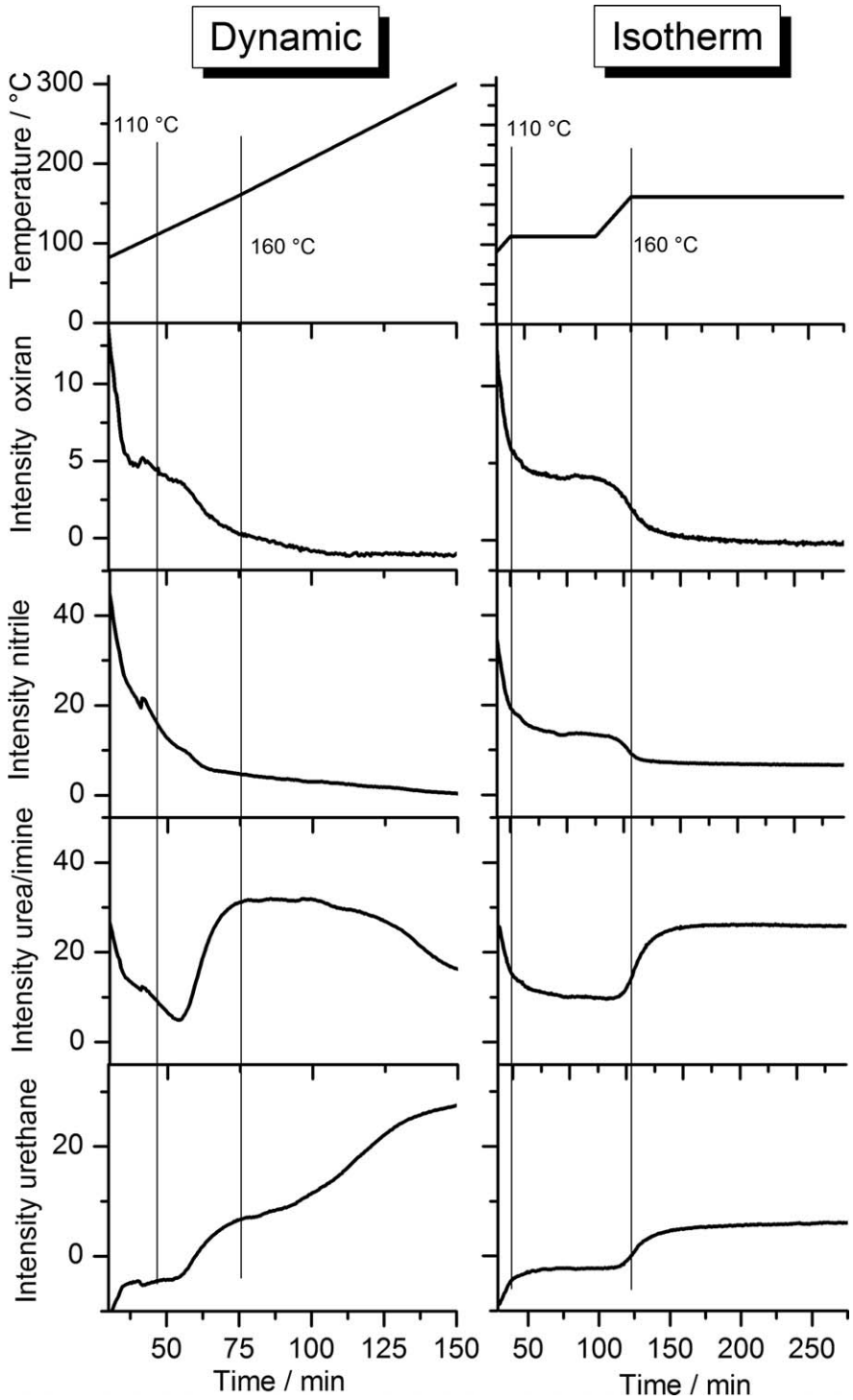

Figure 6. Signal intensities during the curing process, using two different temperature programs. The evaluation parameters are summarized in the middle column of Table II.

imino ether derivative. This reaction will result in a further crosslinking point in addition to the crosslinking point by the oxiran ring reaction. This is the maximum of crosslinking density. At temperatures above 200°C, the urea carbonyls decrease and carbamate carbonyls are formed. This substitution of nitrogen by oxygen at the central carbon atom in the urea derivative can occur only through trans-etherfication reaction by a hydroxyl group. In the literature, a hydrolysis reaction is described instead of this trans-etherfication reaction.[17,19] However, since no water should be present under the conditions of these measurements, we did not consider this reaction. The trans-etherfication results in a bond scission of the crosslinked network of the epoxy resin. A lower network density will result.

Table II. Evaluation Parameters of Curing Process Rates

Identified species	Model mixture from model curing process	Real sample from industrial curing process
Oxiran	927–877	–
Urea carbonyl (+ imine)	1711–1626	1716–1666
Urethane carbonyl	1800–1711 (1800–1551)	1800–1716 (horizontal tangent at 1815 cm^{-1})
Nitrile	2244–2121	2244–2121
Reference signal	–	1938–1832

Integration limits in cm^{-1} (in brackets are the construction points for basis line limits if these are not identical to integration limits).

Characterization of the Real Sample

The results of the model curing process were now correlated with a RS. For this, around 10 parts of a glass-fiber-reinforced component were prepared along the cross section of the temperature gradient (Figure 9 top). Each was measured by FTIR microscope in transmission mode.

Examples of complete spectra are shown in Figure 8, together with spectra of model curing. Due to the presence of glass fibers and the high absorption of infrared light by the Si—O bonds, the spectra cannot be evaluated below 1500 cm^{-1}. This is quite disadvantageous, because the oxiran ring consumption cannot be evaluated. In the spectra of the RS, the nitrile signals can be observed as well as carbonyl and amine signals. The positions of the bands are in good correlation to the signals of the model curing despite the temperature shifts.

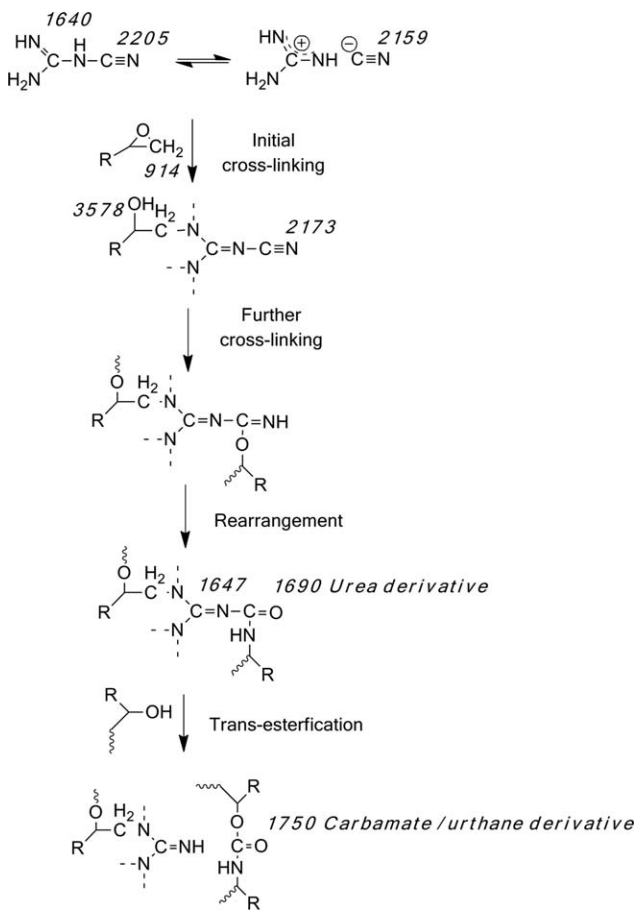

Figure 7. Major curing pathways of the epoxy mixture. For simplification of the schema, only the addition of one oxiran ring at the nitrogen was considered; the further linkages are denoted only by broken lines. The cursive numbers are the observed wavenumbers of the detected species (see text).

However, the comparison of the spectra of RSs with the model curing spectra reveals a heterogeneous result. The nitrile signals in the spectra from the RSs are in the same order of magnitude as the nitrile signals of model curing, but the carbonyl signals are clearly increased.

The spectra of all microtome samples were evaluated according to the evaluation parameters in Table II and plotted against their position in the real specimen (Figure 9). In this evaluation, the sample thickness was considered by dividing the result by an invariant signal (1880 cm^{-1}). The trend of the signals through the cross section of the composite bar shows no clear tendency for the nitrile signal. The disappearance of the double nitrile signal is probably overlapped by the intermediate single signal formed.

However, the urea and carbonyl signals increase in the middle of the sample. According to the results of model, curing this indicates an increased temperature during curing in the middle of sample compared to the positions at the site of the composite part. This effect is also known from the literature.[1,3] It is well known that the low heat conductivity of the glass-fiber-reinforced resin mixture and the exothermic reaction during the curing process will result in inhomogeneous temperature distribution in the bar specimen. It is expected that, from a certain point when the exothermic reaction starts in the middle of the sample, the temperature cannot be dissipated under controlled conditions. As a consequence, the temperature in the middle of sample will exceed the given temperature ranges of the manufacturing tool. According to the proposed curing pathway, the middle of the composite part will be less crosslinked than the outer parts of the composite part.

SUMMARY

In this article, the molecular processes were analyzed that can take place during the curing of an epoxy resin, based on DGEBA and DICY. The single components as well as the non-cured and an oven-cured mixture were investigated by TGA, DSC, and ATR-FTIR measurements, according to their chemical structure and thermal characteristics.

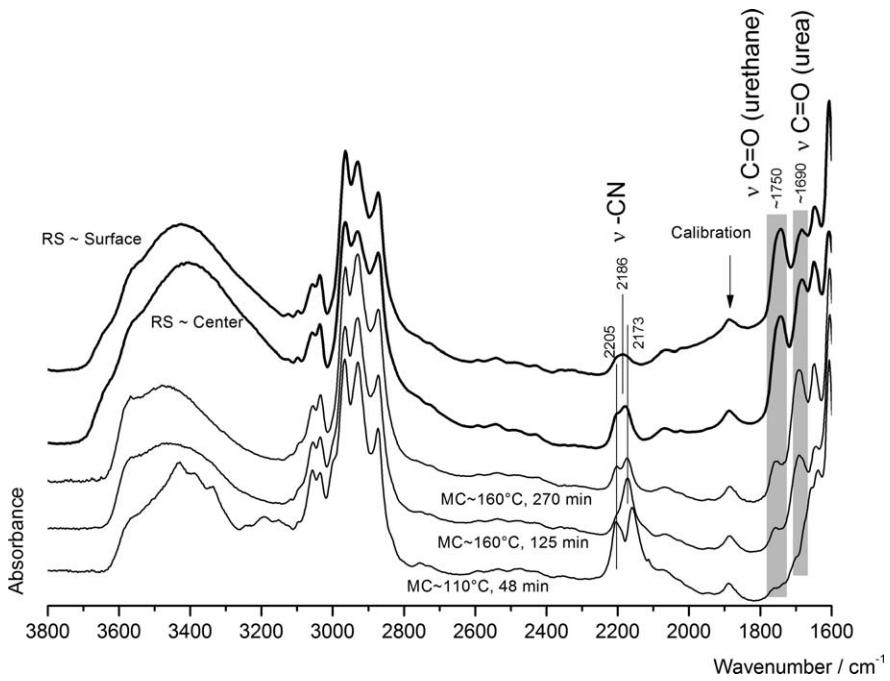

Figure 8. Spectra of real samples (RS) from the epoxy composite bar and comparison to representative spectra from isothermal model curing (MC) of Figure 6 (vertical numbers represent IR absorption frequencies in cm^{-1}).

In situ FTIR measurements in transmission mode were performed with various temperature programs on thin epoxy films. The relevant curing reactions were identified and the influence of temperature on these reactions was investigated. All results were summarized in a chemical reaction pathway schema. A major reaction pathway was postulated, which occurs at temperatures up to 150°C and resulted in a highly crosslinked network. A further reaction pathway takes place at temperatures above 200°C and results in a less crosslinked network and the formation of urethane species.

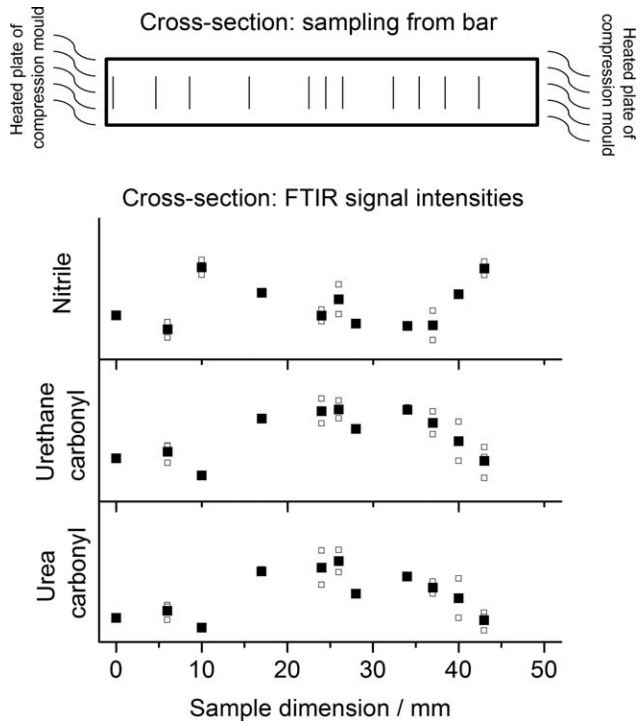

Figure 9. Evaluation of various signal intensities versus sampling position from a real sample (evaluation parameter see Table II). On top, a schema of the sampling geometry is given.

Finally, the results were correlated to a real, industrially cured composite part with a thickness 50 mm. It could be shown that the "high-temperature reaction" pathway took place especially in the middle of the sample. As expected from the model curing, this results in a lower crosslinked density. The inhomogeneous temperature distribution in the bar specimen probably causes this effect, when in the middle of the sample and the temperature of the exothermic reaction cannot be dissipated under controlled conditions.

The final result of this investigation, "Keep the temperature under control in the complete sample," is no surprise for operators of industrial curing processes. The optimization of curing temperatures for complex epoxy specimens is a topic of various, large-scale tests to increase durability and reduce process costs. But in contrast to this practical optimization, we were able to formulate the molecular reactivity behind this phenomenon and contribute to its understanding.

ACKNOWLEDGMENTS

The authors thank D. Neubert, G. Teteris, and E. Lorenz for their assistance with TGA and DSC measurements as well as sample preparation by microtome. Furthermore, they thank V. Trappe from BAM and M. Voigt from IFC composite for helpful discussions. They also thank the AiF Projekt GmbH for its financial support of the research work on project KF2201036CK1.

REFERENCES

1. Michaud, D. J.; Beris, A. N.; Dhurjati, P. S. *J. Compos. Mater.* **1998**, *32*, 1273.
2. Rath, M.; Döring, J.; Stark, W.; Hinrichsen, G. *NDT & E Int.* **2000**, *33*, 123.
3. Oh, J. H.; Lee, D. G. *J. Compos. Mater.* **2002**, *36*, 19.
4. Eyerer, P. *J. Appl. Polym. Sci.* **1971**, *15*, 3067.
5. Enns, J. B.; Gillham, J. K. *J. Appl. Polym. Sci.* **1983**, *28*, 2567.
6. Munz, M.; Sturm, H.; Stark, W. *Polymer* **2005**, *46*, 9097.
7. Rabearison, N.; Jochum, C.; Grandidier, J. C. *J. Mater. Sci.* **2011**, *46*, 787.
8. Trappe, V.; Günzel, S.; Jaunich, M. *Polym. Test.* **2012**, *31*, 654.
9. George, G. A.; Cash, G. A.; Rintoul, L. *Polym. Int.* **1996**, *41*, 169.
10. Luda, M. P.; Balabanovich, A. I.; Zanetti, M.; Guaratto, D. *Polym. Degrad. Stab.* **2007**, *92*, 1088.
11. Sánchez-Soto, M.; Pagés, P.; Lacorte, T.; Briceño, K.; Carrasco, F. *Compos. Sci. Technol.* **2007**, *67*, 1974.
12. Mounif, E.; Bellenger, V.; Tcharkhtchi, A. *J. Appl. Polym. Sci.* **2008**, *108*, 2908.
13. Cruz, J. C.; Osswald, T. A. *Polym. Eng. Sci.* **2009**, *49*, 2099.
14. Poisson, N.; Lachenal, G.; Sautereau, H. *Vib. Spectrosc.* **1996**, *12*, 237.
15. Lin, R.-H. *J. Polym. Sci. Part A: Polym. Chem.* **2000**, *38*, 2934.
16. Pitt, J. J.; Pearce, P. J.; Rosewarne, T. W.; Davdson, R. G.; Ennis, B. C.; Morris, C. E. M. *J. Macromol. Sci. Part A: Chem.* **1982**, *17*, 227.
17. Gilbert, M. D.; Schneider, N. S.; MacKnight, W. J. *Macromolecules* **1991**, *24*, 360.
18. Hong, S.-G.; Wu, C.-S. *Thermochim. Acta* **1998**, *316*, 167.
19. Gundjian, M.; Cole, K. C. *J. Appl. Polym. Sci.* **2000**, *75*, 1458.
20. Gao, Y.; Yu, Y. *J. Appl. Polym. Sci.* **2003**, *89*, 1869.
21. Liu, X. D.; Sudo, A.; Endo, T. *J. Polym. Sci. Part A: Polym. Chem.* **2011**, *49*, 250.
22. Liu, X. D.; Kimura, M.; Sudo, A.; Endo, T. *J. Polym. Sci. Part A: Polym. Chem.* **2010**, *48*, 5298.